WOOD RESEARCH doi.org/10.37763/wr.1336-4561/66.4.595605
e-ISSN 2729-8906
66(4): 2021 595-605 pp.

TRACE ELEMENT ANALYSIS OF TROPICAL WOODS USING PARTICLE INDUCED X–RAY EMISSION (PIXE) METHODS FROM WESTERN NIGERIA

CHARITY ADAEZE ONUMEJOR
COVENANT UNIVERSITY
NIGERIA

FATAI AKINTUNDE BALOGUN, SEJLO TEMIDAYO GBENU
OBAFEMI AWOLOWO UNIVERSITY
NIGERIA

MOJISOLA RACHAEL USIKALU, THEOPHILUS AANUOLUWA ADAGUNODO, AKINWUMI AKINPELU, JUSTINA ADA ACHUKA, THEOPHILUS EMUOBOR ARIJAJE
COVENANT UNIVERSITY
NIGERIA

(RECEIVED JULE 2020)

ABSTRACT

Trace element investigation and its corresponding concentration level in selected tropical woods from western Nigeria was done using PIXE-particle induced X-ray emission methods. Fifteen selected tropical woods were analyzed and twenty-seven trace elements were identified and quantified. The identified trace elements are Na, Mg, Al, Si, P, S, Cl, K, Ca, Ti, V, Cr, Mn, Fe, Co, Ni, Cu, Zn, Se, Br, Rb, Sr, Y, Zr, Ba, Pb and Bi. Calcium concentration were 2835, 3195, 4923, 5608, 7770, 5110, 2743, 5092 and 3451 ppm in samples 2, 5, 6, 10, 11, 12, 13, 14 and 15, respectively. Potassium recorded 2838, 4811, 3184, and 2021ppm in samples 1, 3, 8 and 9, respectively. Silicon recorded 5206 ppm for sample 4 and 5253 ppm for sample 7. Calcium and potassium were observed to have concentration level that is greater than 1000 ppm in all the studied samples, hence it can be said that calcium and potassium are major trace element of wood. The concentrations of the elements identified have no immediate health concern on environment and human, therefore the studied tropical woods safe for use as fuel and other purposes.

KEYWORDS: Wood elemental composition, wood elemental constituents, Particle induced X-ray emission method (PIXE), trace element analysis, Ion beam analysis (IBA).

INTRODUCTION

Particle induced X-ray emission (PIXE) is one of the Ion beam analytical (IBA) methods that detect elements with high atomic number $Z \geq 11$ in samples based on atomic fluorescence. In general, IBA methods are used to study materials of complex elemental matrix, based primarily on interaction between the samples elemental constituent and accelerated charged particle. Study samples are bombarded with charged particle to induce such interaction. Other IBA techniques are Particle induced gamma-ray emission (PIGE), Nuclear reaction analysis (NRA), and Rutherford backscattering spectrometry (RBS). PIGE and NRA are based on nuclear reactions while RBS is based on ion beam scattering techniques (Beck 2005). Many thin film composition analysis, optical coatings and depth profiling primarily make use of RBS. Many researches on elemental composition of materials (samples) employs destructive methods or digestion processes for the elemental analysis. Only every few research go for non-destructive analytical methods such as those of ion beam analytical techniques (Okochi 2007, Onumejor et al. 2018). This informed the use of Particle induced X–ray emission (PIXE) methods for trace element analysis of tropical wood from Western Nigeria. The knowledge of elemental constituents of any material serves as foundation for other numerous scientific findings about that sample material and their possible contribution to background environmental health or radioactivity (Xinwei 2006, Felix et al. 2013, Usikalu et al. 2018, Orosun et al. 2019, Joel et al. 2018, Adagunodo 2018). Therefore, knowing the elemental constituents of tropical woods will tell a lot about its other scientific usefulness. Woods are popularly used as fuel and furniture. Scientists have found other uses of wood that are of immerse benefit to humans, especially in the medical field. Bradley et al. (1991) worked on the photon attenuation potentials of tropical hardwoods and linked his findings to uses of woods in medicine. Scientists Zhang et al (2010), Constantinou (1982), White (1977) and Požgaj (1977) did some studies on the dosimetric usefulness of woods; its property, as combustible heat source and as medical phantom in radiotherapy. Tajuddin et al. (1996) reported the scattering investigation and radiographic properties of Rhophoraspp hardwood, its suitability as phantom material for dosimetric study. The value of woods and possible scientific uses all began with the simple knowledge of elemental composition. This prompted scientist in African region with rich tropical wood territory to conduct elemental studies and publish their discoveries. Aggrey-Smith (2015), measured the elemental compositions of some tropical wood species from pra-anum forest in Ghana using Instrumental neutron activation analysis (INAA). Zafar (2010) and Sakina (2013) also highlighted the importance of elemental analysis of wood/herbs for medicinal purposes. The present study will give details of trace elemental constituent of fifteen tropical woods from Western Nigeria using particle induce X-ray emission (PIXE) method. Recent research works on use of hardwood in other field of studies such as engineering (Haradhan and Chun, 2020, Sarmad et al. 2020, Chu et al. 2020) arts (Yasuji et al. 2020), medicine (Sachithrani et al. 2020, Assai et al. 2020), agriculture (Dora et al. 2020, Dominik et al. 2020), environmental management (Tejedor et al. 2020, Achim et al. 2020, Warlen et al. 2020), technology (Mátyás et al. 2020, Erchiqui et al, 2020),

communication (Qian et al. 2020, Yuming et al. 2020), reveals the diverse ways that wood analysis can be manipulated to serve multiple purposes.

MATERIAL AND METHODS

Sample preparation

A total of 15 tropical woods were selected for this study, from the western part of Nigeria, as shown in Tab. 1. Identification and collection of wood samples was done in collaboration with trained personnel from FRIN-Forest Research Institute of Nigeria, Ibadan. Selection criteria were based on availability, easy access, abundance and possibility of cultivation. The harvested wood samples were cut into small pieces, peeled, sun dried and grinded. Sun drying lasted for 14 weeks. 2 mm mesh size sieved was used for wood powders sieving after grinding. The wood powders were pelletized at pressing pressure of 8 metric tons gauge readings using hydraulic press at the Center for Energy Research and Development (CERD) measurement laboratory, Obafemi Awolowo University, Ile-Ife, Ogun State, Nigeria. Sample pellets weight ranged from 250 mg to 350 mg. Each wood sample pellet was placed in properly labeled dispensary bags and taken to the PIXE laboratory at CERD for elemental analysis. GupixWin software program was used for PIXE Spectrum analysis, The PIXE results were obtained in PPM (part per million) (Futatukawa 2000).

Tab. 1: Wood sample IDs, botanical and common names (Onumejor et al. 2018).

Sample ID	Botanical names	Local or common names
1	*Treculia africana*	Afon
2	*Triplochiton scleroxylon*	Arere (Obeche)
3	*Albizia zygia*	Aynure-white or Ayunre
4	*Albizia gummifera*	Aynure or Ayunre-yellow
5	*Cedrella odorata*	Cidrela
6	*Basella alba*	Efo-onibo
7	*Anadelphia afzeliana*	Bere
8	*Gmelina arborea*	Gmelina
9	*Funtumia spp elastic*	Ire
10	*Milicia excels*	Iroko
11	*Blahia sapida*	Isin
12	*Celtis spp*	Ita
13	*Irvingia grandifolia*	Kara koro
14	*Senna siamea*	Kasia
15	*Mansonia altissima*	Masonia

Description of accelerator facility for PIXE analysis

The accelerator facility used for this research is NEC 5SDH 1.7 MV Accelerator machine model at the Center for Energy Research and Development (CERD), Obafemi Awolowo University Ile-Ife. The ion beam analytical processes are situated inside the accelerator close to the radiofrequency (RF) charge exchange ion source. The helium and proton ions that are used to bombard research samples are generated from the ion source chamber. The accelerator facility has five ion beam lines, but only one beam line with multipurpose end station is active.

This end station has four functional IBA techniques that it can run. The IBA that the accelerator facility can run techniques includes Particle induced gamma ray emission (PIGE), Elastic recoil detection analysis (ERDA), Rutherford backscattering spectrometry (RBS) and Particle induced X-ray emission (PIXE). Each are stationed at 225^o, 30^o, 165^o and 135^o respectively. The window for beam size and position observation is at 0^o. In PIXE technique, only the top area of the sample, about 10-50 μm deep is probed by the incident charge ion beam. The profiling depth depends on the energy of the incident beam and the type of sample material. Usually the bombarded sample area for PIXE analysis is a circular section of the sample that is about 1-10mm in diameter. Therefore, the small area must be a complete representation of the whole sample, hence the pulverization (grinding) and pelletizing of the wood samples used for this study was done (Mingay 1983, Ishii 1990, Mandó 1994).

PIXE detector calibrations

Commercially available standards were used for PIXE detector calibrations. The thin mylar foils and Hey types of micromatter standards used for this study has compound/element deposits of known concentration. These micromatter standards were first analyzed using the PIXE setup process before analyzing the study samples. Results of the standards obtained were checked and compared with stated concentration on purchase specification within error margin of five percent as state by Mingay (1983), Ishii (1990) for X-ray detector calibrations. In calibrating the system, the 0.6 - 3.5 MeV energy ranges of the $4He^+$ particles were used to bombard the standard samples. The choice of commercial standard selected are such that provide a representation of the entire spectrum needed for the analysis.

Applications of PIXE to elemental analysis

Collimator was positioned in front of the target, and the beam spot was resized to 1mm. When beam hits the target, the X-ray detector collects and measure X-ray from target (study samples) by analyzing the energy spectrum using equation 1. Obtained counts $N_x(Z)$ and atomic number Z of the characteristic X-rays for each detected element were automatically substituted and analyze with GUPIXWIN software.

Mounting a sample uniformly on a thin polyethylene film, we obtain the quantity NZ ($g \cdot cm^{-2}$) for element Z as follows:

$$N_Z = N_X(Z)\frac{4\pi m_Z z_p e}{\sigma_Z^X d\Omega e f f_Z Q N_{Av.}} \quad (1)$$

where: dΩ, ef, f_Z, Q, z_P and N_{Av}. are the solid angle of the X-ray detector, the detector efficiency, integrated projectile charge, projectile charge, and Avogadro's number respectively.

In the case of a thick target, the effect of the reduction due to the X-ray self-absorption and projectile energy loss in the target should be considered when applying the above formula. (Keizo 2019, Ishii 2019).

RESULTS AND DISCUSSION

Study samples were analyzed under the same experimental procedures as those of the micromatter commercial standards used for calibration. Micromatter standards has certified values used to validate the PIXE procedure. GUPIXWIN spectrum analysis software was used for identification of characteristic X-rays through their energies and quantitative analysis of their subsequent elemental concentrations. A total of 27 trace elements were identified and quantified in part per million concentration levels as shown in Tab. 2.

Tab. 2: PIXE elemental concentrations of selected samples 1 to 15 ($\mu g.g^{-1}$).

Elements	Sample ID														
	1	**2**	**3**	**4**	**5**	**6**	**7**	**8**	**9**	**10**	**11**	**12**	**13**	**14**	**15**
Na	389	0	65.35	0	68.03	0	245.8	125.8	0	48.95	0	0	0	125	0
Mg	2653	33.41	536	294.3	1178	1198	719.1	1508	1075	1504	683.6	187.8	742.3	474	930.9
Al	268.7	158.1	368	85.4	338.4	667.5	262.2	337.9	296.5	483.9	452.2	258.2	301.6	130.5	435.3
Si	441	276	645.8	5206	512.9	1509	5253	543.3	342	795.3	615.1	458.3	713.6	318.7	430.8
P	201.9	52.32	99.61	252.6	0	342.5	275.5	57.88	286.1	0	397.3	93.1	301.4	186.9	381.3
S	697.8	220.3	714.5	1171	214.8	718.5	278.3	61.29	694.1	95.19	605.8	218.2	666.8	188.4	210.1
Cl	146.9	227.8	84.33	511.3	57.56	35.16	2768	2.996	31.63	87.36	38.41	80.8	68.42	75.23	48.38
K	2838	1925	4811	1489	1096	2001	3487	3184	2021	2362	2139	1364	1106	2331	1809
Ca	1524	2835	2082	846.1	3195	4923	3192	2857	1996	5608	7770	5110	2743	5092	3451
Ti	7.6	2.619	9.945	2.345	0	10.82	2.386	11.28	0	7.632	10.51	2.745	9.618	8.532	13.65
V	5.504	2.523	0	3.437	0	1.763	3.702	0	0	0	5.534	0	4.152	0.5542	0
Cr	6.477	2.913	0	0	1.935	4.565	5.887	0	0.8619	0	0	0	2.184	0	4.591
Mn	17.29	1.592	19.97	10.89	0	9.832	8.443	2.833	14.64	8.742	24.64	7.324	60.33	3.817	0
Fe	18.26	75.99	109.5	1851	36.81	209.6	21.59	833.3	22.11	68.39	91.98	26.86	34.21	15.29	28.99
Co	6.656	0	0.9216	36.67	6.369	0	10.1	8.867	0	9.798	0	0	0.2863	4.786	5.281
Ni	0	0	0	9.541	4.08	10.7	1.377	0.8991	0	0	0	0	2.622	2.328	0
Cu	2.077	6.352	2.606	8.026	0	1.443	0	0	7.7	4.93	5.892	2.867	1.287	11.24	1.962
Zn	40.08	3.43	11.57	0	1.762	45.96	8.786	22.4	19.64	1.156	31.81	10.33	11.65	4.664	0
Se	5.636	0	0	0	0	0	0	0	2.971	0	0	0	0	0	0
Br	0	3.015	0	50.75	5.844	5.061	0	3.164	0	2.829	0	13.46	6.253	0	4.803
Rb	25.65	15.94	0	18.12	10.94	13.77	0	0	0	0	12.18	37.97	0	8.996	0
Sr	0	33.35	22.65	0	37.17	0	0	0	0	158.5	160.3	96.88	20.29	75.11	27.82
Y	0	0	16.62	25.35	14.57	0	0	14.65	0	29.65	0	0	0	0	14.72
Zr	0	69.71	0	70.92	0	0	61.02	70.82	13.75	0	0	35.68	35.66	0	0
Ba	0.6211	3.804	0.6734	0	0	8.03	6.138	7.411	0.8325	12.42	3.085	4.512	7.527	0	0.3293
Pb	1.258	1.149	0.362	8.189	1.76	0.6914	0	0	1.225	1.015	0	0	0	0	0
Bi	3.543	0	0	5.518	0.7421	0.8008	0	0	0.9968	0	0.358	0	0	0	0.4648

The identified trace elements are Na, Mg, Al, Si, P, S, Cl, K, Ca, Ti, V, Cr, Mn, Fe, Co, Ni, Cu, Zn, Se, Br, Rb, Sr, Y, Zr, Ba, Pb and Bi. Silicon Si, Potassium K and Calcium Ca, Magnisium Mg, recorded the highest in several sample. Calcium had the highest concentration values in 9 different samples, Potassium in 4 and Silicon in 2 samples. Calcium had 2835, 3195, 4923, 5608, 7770, 5110, 2743, 5092 and 3451 ppm in samples 2, 5, 6, 10, 11, 12, 13, 14 and 15, respectively. Potassium had 2838, 4811, 3184, and 2021 ppm in samples 1, 3, 8 and 9, respectively. Silicon has 5206 ppm in sample 4 and 5253 ppm in sample 7. To better identify the major trace element in studied samples, a cumulative distribution pattern plot of trace

element was done as shown in Fig. 1. The lines with label 1000 to 8000 represents trace elements concentration levels in ppm, the digits 1 (one) to 15 (fifteen) on the concentration line edges represents the 15 (fifteen) studied samples. Each identified and quantified trace element were represented with several colored lines as shown on the legend in Fig. 1. The four noticeable patterns above the 1000 ppm concentration line, represents the major trace element measured in studied samples. Calcium Ca, with grey colored line, formed the largest pattern, its highest concentration level points to 11 as shown in Fig. 1.

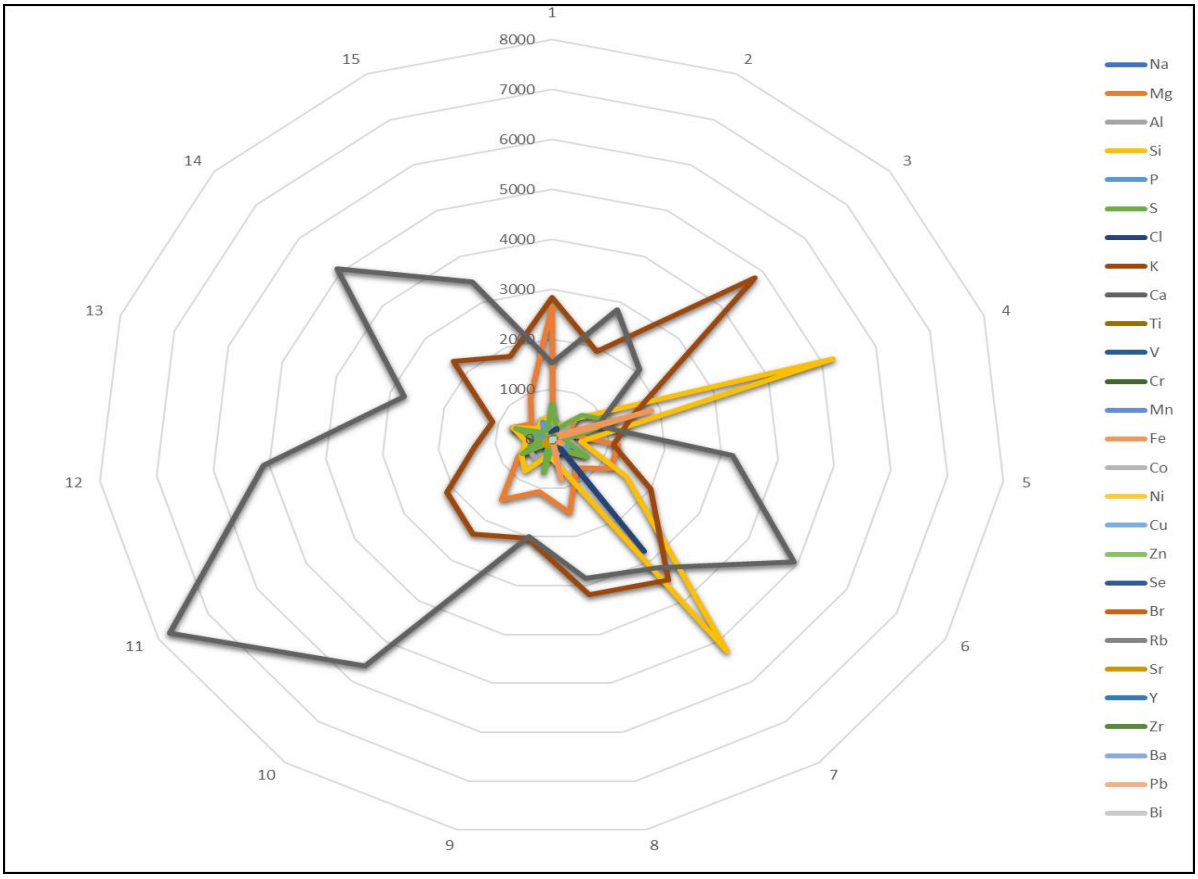

Fig. 1: Radar plot of cumulative distribution pattern of trace element in studied samples.

Next large pattern observed was Potassium K, with red colored line and highest trace element concentration points edge is on 3 (sample 3). The yellow colored line pattern with point edges on samples 4 and 7 stands for Silicon Si distribution. Magnesium Mg, with orange colored line was the fourth noticeable pattern with highest concentration edge point on sample 1. Other trace element distribution patterns were clustered below the 1000 ppm concentration line. Hence, it can be said that Calcium Ca, Potassium K, Silicon Si, and Magnesium Mg, were the major trace element of studied wood samples. Other elements that can be included as major trace elements are those present in all studied samples. They are Al, P, S, Cl, Mn, Fe, and Zn. This implies that Calcium Ca, Potassium K, and Silicon Si are the major trace elements of the studied wood samples, having concentration levels > 1000 ppm. Fig. 2, revealed that the detected trace elements clustered around Na to Ca, as shown on the x-axis (trace element axis) position 1 to 9. The observed concentration order were Ca < K < Si < Mg < others.

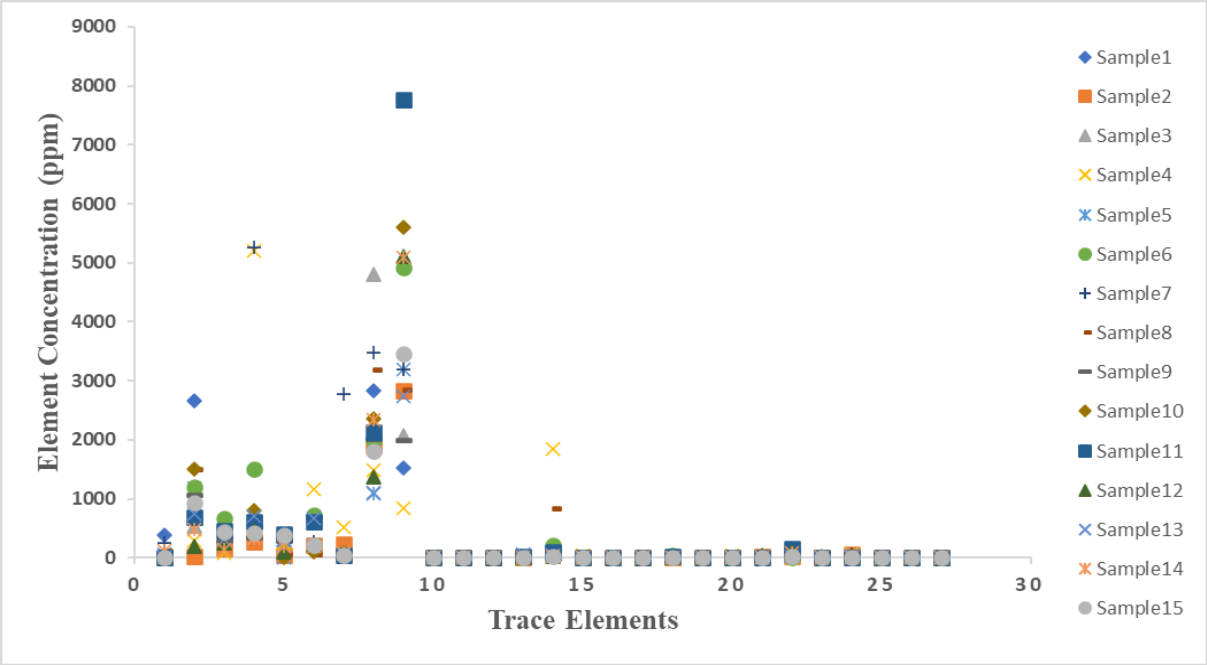

Fig. 2: Trace elemental concentration of samples.

CONCLUSIONS

Fifteen different types of tropical wood were studied using particle induce X-ray emission (PIXE) method of ion beam analytical techniques, for identification of constituent elements and its corresponding concentration level in ppm. Elements identifies with varying concentration levels are Na, Mg, Al, Si, P, S, Cl, K, Ca, Ti, V, Cr, Mn, Fe, Co, Ni, Cu, Zn, Se, Br, Rb, Sr, Y, Zr, Ba, Pb and Bi. Calcium had 2835, 3195, 4923, 5608, 7770, 5110, 2743, 5092 and 3451 ppm in samples 2, 5, 6, 10, 11, 12, 13, 14 and 15 respectively. Potassium had 2838, 4811, 3184, and 2021 ppm in samples 1, 3, 8 and 9 respectively. Silicon has 5206 ppm for sample 4 and 5253 ppm for sample 7. Many elements were below detection limit and were reported to have zero concentration values in the result tables. Calcium and potassium were observed to have concentration level that is greater than 1000 ppm in all the studied samples, hence it can be said that calcium and potassium are major trace element of wood. The concentrations of the elements identified have no immediate health concern and is therefore safe for use as fuel and other purposes.

ACKNOWLEDGMENTS

We appreciate the management of Covenant University, Nigeria for the publication support received from them.

REFERENCES

1. Beck, L., 2005: Improvement in detection limits by using helium ions for particle-induced X-ray emission. X-Ray Spectrom 34: 393–399.
2. Okochi, T., Hoshino, Y., Fujii, H., Mitsutani, T., 2007: Nondestructive tree-ring measurements for Japanese oak and Japanese beech using micro-focus X-ray computed tomography. Dendrochronologia (online) 24(2-3): 155-164.
3. Onumejor, C.A., Balogun, F.A., Akinpelu, A., Arijaje, T.E., Usikalu, M.R., 2018: Rutherford backscattering spectrometry (RBS) method for the determination of elemental constituent of tropical wood matrices from Western Nigeria. IOP Conf. Series: Earth and Environmental Science 173: 1-4.
4. Xinwei, L., Zhang, X., 2006: Measurements of natural radioactivity in sand collected from the Baoji Weihe Sands Park, China. Environmental Geology 50: 977-982.
5. Olise, F.S., Onumejor, C.A., Akinlua, A., Owoade, O.K., 2013: Geochemistry and health burden of radionuclides and trace metals in shale samples from the North-Western Niger Delta Journal of Radioanalytical and Nuclear Chemistry 295: 871–881.
6. Usikalu, M.R., Onumejor, C.A., Akinpelu, A., Achuka, J.A., Omeje, M., Oladapo, O.F., 2018: Natural radioactivity concentration and its health implication on dwellers in selected locations of Ota. IOP Conf. Series: Earth and Environmental Science 173: 1-8.
7. Orosun, M.M., Usikalu, M.R., Oyewumi, K.J., Adagunodo, A.T., 2019: Natural radionuclides and radiological risk assessment of Granite mining field in Asa, North-Central Nigeria. MethodsX 6: 2504-2514.
8. Joel, E.S., Maxwell, O., Adewoyin, O.O., Ehi-Eromosele, C.O., Embong, Z., Oyawoye, F., 2018: Assessment of natural radioactivity in various commercial tiles used for building purposes in Nigeria. MethodsX 5: 8-19.
9. Adagunodo, T.A., George, A.I., Ojoawo, I.A., Ojesanmi, K., Ravisankar, R., 2018: Radioactivity and radiological hazards from a kaolin mining field in Ifonyintedo, Nigeria. MethodsX 5: 362–374.
10. Bradley, D.A., Tajuddin, A.A., Sudin, C.W.A.C.W., Bauk, S., 1991: Photon attenuation studies on tropical hardwoods. International Journal of Radiation Applications and Instrumentation. Part A. Applied Radiation and Isotopes 42771-773.
11. Zhang, X., Chen, Q., Bradford, R., Sharifi, V., Swithenbank, J., 2010: Experimental investigation and mathematical modelling of wood combustion in a moving grate boiler. Fuel Processing Technology 91(11): 1491-1499.
12. Constantinou, C., 1982: Phantom materials for radiation dosimetry, I. liquids and gels. British Journal of Radiology: 52217-224.
13. White, D.R., 1977: An analysis of the Z-dependence of photon and electron interactions. Physics in Medicine and Biology 22(1977b): 219-228.
14. Požgaj, A., Chovanec, D., Kurjatko, S., Babiak, M., 1997: Structure and properties of wood (in Slovak). Príroda a.s., Bratislava, 485 pp.

15. Tajuddin, A.A., Sudin, C.W.A.C.W., Bradley, D.A., 1996: Radiographic and scattering investigation on the suitability of *Rhizophora* spp. as tissue-equivalent medium for dosimetric study. Radiation Physics and Chemistry 47: 739-740.
16. Aggrey-Smith, S., Preko, K., Wilson, F., Gbadago, J., 2015: Measurement of elemental compositions of selected tropical wood species – a case study of Pra Anum Forest, Ghana. International Journal of Biomedical Science and Engineering 3(3): 34-43.
17. Zafar, A.M, Mohammad, S, Saad Bin, Z.M, Mahwish, A.K., 2010: Herbal treatment for cardiovascular disease. The evidence-based therapy. Pakistan Journal of Pharmaceutical Sciences 23(1): 119-124.
18. Sakina, M.Y., Alia, E.A.R., Gihan, O.M.E., Abdelhafeez, M.A.M., 2013: Elemental analysis of ten Sudanese medicinal plants using X-ray fluorescence. Journal of Applied and Industrial Sciences 1(1): 49-53.
19. Futatukawa, S., 2000: Bio PIXE theory and applications. Chapter 2. Sample preparation for the quantitative analysis of biological materials. Sample preparation method of biological materials by Nitric Acid ashing using a Microwave Oven. Radioisotopes 49: 447–450.
20. Mingay, D., 1983: Calibration of micromatter co. Standards used for the calibration of PIXE analysis systems. Journal of Radioanalytical Chemistry, (Foils manufactured by Micromatter Co., Deer Harbor, WA.) 78: 127.
21. Ishii, K., Morita, S., 1990: Bio-PIXE at the Takizawa facility (Bio-PIXE with a baby cyclotron). International Journal of PIXE 1: 1–29.
22. Mandó, P.A., 1994: Advantages and limitations of external beams in applications to arts & archeology, geology and environmental problems. Nuclear Instruments and Methods B 85: 815–823.
23. Keizo, I., 2019: PIXE and its applications to elemental analysis. Quantum Beam Science 3(2): 12.
24. Ishii, K., Terakawa, A., Ushijima, H., Hitomi, K., Nagano, N., Nogami, M., 2019: Application of a medical PET cyclotron to PIXE analysis. In: Proceedings of the 16th International Conference on Particle Induced X-ray Emission. Pp 39-40, vol. 39, Caldas da Rainha, Portugal.
25. Haradhan, K., Chun W.K., 2020: High acoustic absorption properties of hackberry compared to nine different hardwood species: a novel finding for acoustical engineers. Applied Acoustics 169: 1-8.
26. Sarmad, S., Luigi, F., Raffaele L., 2020: Behavior factor evaluation of CFS wood sheathed shear walls according to FEMA P695 for Eurocodes. Engineering Structures 221: 2-8.
27. Chu, P., Ashraf, A.D., Ahmed, M.A.H., 2020: Simplified numerical approach for the lateral load analysis of light-frame wood shear wall structures. Engineering Structures 219: 1-7.
28. Yasuji, K., Shigeru, Y., Tsutomu, T., Yoichi, S., 2020: Coloring mechanisms of ancient buried wood: Japanese cedar trees excavated from the foothills of Mt. Chokai. Journal of Wood Science 66: 1-7.
29. Sachithrani, K., Sachinthani, K., Lahiru, R., Kalpani, A., Disnie, R., Hashan, J., Cholani, W., Suneth, S., 2020: Assessment of the applicability of wood anatomy and DNA

barcoding to detect the timber adulterations in Sri Lanka. Pp. 5-10, Scientific Reports, vol. 10.
30. Assai, H., Paul, H., Hussam, M., 2020: Structural performance of a wood-sand-wood wall for blast protection. Engineering Structures 219: 1- 9.
31. Dora, N., Sibylle, F., Rainer, G.J., 2020: Characterization of charcoal and firewood ash for use in African peri-urban agriculture. Chemical and Biological Technologies in Agriculture 7: 1-8.
32. Dominik, T., Andreas, S., Julius, S., Jonas, H., Jörg, M., Rupert, S., 2020: Effects of disturbance patterns and deadwood on the microclimate in European beech forests. Agricultural and Forest Meteorology 291: 1-10.
33. Tejedor, J., Cóndor, V., Almeida-Naranjo, C.E., Guerrero, V.H., Villamar, C.A., 2020: Performance of wood chips/peanut shells biofilters used to remove organic matter from domestic wastewater. Science of The Total Environment 738: 3-5.
34. Achim, B., Marek, W., Andreas L., Doris, G., Michał, W., 2020: Petrological and geochemical characteristics of xylites and associated lipids from the First Lusatian lignite seam (Konin Basin, Poland): Implications for floral sources, decomposition and environmental conditions. Organic Geochemistry 147: 3-7.
35. Warlen, S. C., Maura, D.C., Pablo, J.F., Pena, R., Marianade, A.I., Fernando, V., Claudia, F.B., 2020: Intraspecific variation in functional wood anatomy of tropical trees caused by effects of forest edge. Forest Ecology and Management 473: 1-11.
36. Mátyás, B., Róbert. N., Jakub, S., Anna, S., 2020: FTIR analysis of chemical changes in wood induced by steaming and longitudinal compression. Cellulose 27: 6811-6829.
37. Erchiqui, F., Kaddami, H., Dituba-Ngoma, G., Slaoui-Hasnaoui, F., 2020: Comparative study of the use of infrared and microwave heating modes for the thermoforming of wood-plastic composite sheets. International Journal of Heat and Mass Transfer 158: 1-9.
38. Qian, H., Tianyi, Z., Haiyang, Z., Zehui, J., Lu, H., Xiaoning, L., 2020: Prediction of stiffness and strength distributions in laminated-wood treated by high voltage electrostatic field (HVEF). Materials Today Communications 24: 1-11.
39. Yuming, X.Y., Huanga, X., Menga, F., Wangb, L., Wana, Z., Donga, J.C., 2020: Friction rivet joining towards high-performance wood-metal hybrid structures. Composite Structures 247: 1-7.

CHARITY ADAEZE ONUMEJOR*, MOJISOLA RACHAEL USIKALU, THEOPHILUS AANUOLUWA ADAGUNODO, AKINWUMI AKINPELU, JUSTINA ADA ACHUKA, THEOPHILUS EMOBOR ARIJAJE
COVENANT UNIVERSITY
DEPARTMENT OF PHYSICS
P.M.B 1023
OTA, OGUN STATE
NIGERIA
*Corresponding author: charity.onumejor@covenantuniversity.edu.ng

FATAI AKINTUNDE BALOGUN, SEJLO TEMIDAYO GBENU
OBAFEMI AWOLOWO UNIVERSITY
CENTRE FOR ENERGY RESEARCH AND DEVELOPMENT
P.M.B. 13
ILE-IFE, OSUN STATE
NIGERIA